DOI: 10.1002/chem.200601739

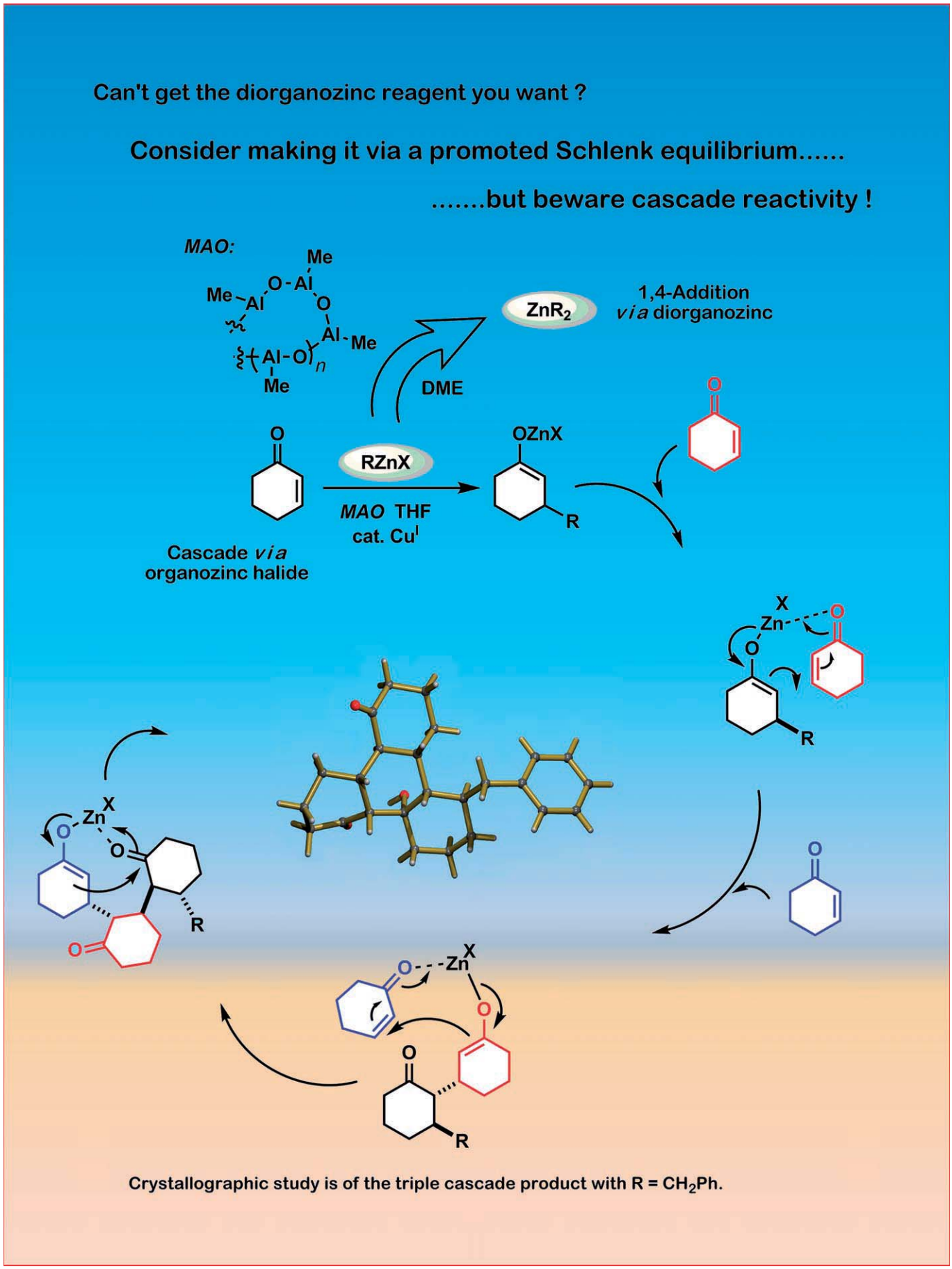

Demonstration of Promoted Zinc Schlenk Equilibria, their Equilibrium Values and Derived Reactivity

Alexander J. Blake, Jonathan Shannon, John C. Stephens, and Simon Woodward*[a]

Abstract: The presence of promoted Schlenk equilibria for organozinc halide species has been explicitly demonstrated by ^{13}C NMR studies. Thus, addition of methylaluminoxane $(MeAlO)_n$, MAO, to RZnX (R = Et, Bn, $ArCH_2$, $(CH_2)_3CO_2Et$; X = Cl, Br) leads to the formation of ZnR_2 and ZnX_2·MAO. For EtZnCl, equilibration of $ZnEt_2$ and ZnX_2·MAO is rapid at −35 °C; a K value of 0.19 M^{-1} indicates the equilibrium favours $ZnEt_2$ (0.75–3.0 equiv MAO). Use of RZnX/MAO mixtures allows copper-catalysed 1,4-addition to 2-cyclohexenone to be achieved, but a competing cascade reaction (two subsequent Michael additions and an intramolecular aldol reaction) leads to novel tetracyclic by-products (characterised crystallographically in one case). Activation of EtZnCl is also achieved by $ZnMe_2$ addition and the presence of intermediate EtZnMe was observed by ^{13}C NMR spectroscopy (at equilibrium, $K \approx 1$). Asymmetric conjugate addition in this system can be realised (up to 92 % *ee* for additions to 2-cyclohexenone).

Keywords: aluminum · diorganozinc · organozinc halide · Schlenk equilibria · structure elucidation · zinc

Introduction

Recently we described S_N2' displacement of the allylic chloride **1**, and related species, in which $ZnEt_2$ leads to highly stereoselective formation of **2** (Scheme 1).[1]

The use of a methylaluminoxane [$(MeAlO)_n$, MAO] additive was crucial to the realisation of high *ee* values in these reactions. It was postulated that removal of the kinetic EtZnCl by-product (which leads to unselective S_N2' reactions) by MAO was instrumental in achieving this. Similar observations were made by using $ZnMe_2$ as an apparent halide scavenger (**2** generated in 84 % *ee*). The success of these approaches implied that the zinc Schlenk equilibrium [Eq. (1)] was being modified in processes that can be represented by equilibria shown in Equations (2) and (3). Although the suggestion has been made that the equilibrium constant for the formation of ZnR_2 in the unpromoted zinc Schlenk case [Eq. (1)] is vanishingly small,[2] essentially nothing is known about such processes.[3] As an alternative, one could suggest that the observed reactivity in Scheme 1 is due simply to the presence of the Lewis acids MAO and $ZnMe_2$, which activate substrate **1** to a point at which the RZnX species become adequate nucleophiles.[4] It is therefore important to demonstrate explicitly that the equilibria shown in Equations (2) and (3) do operate, to measure their equilibrium constants and to show other catalytic procedures that could also use this new approach for ZnR_2 formation.

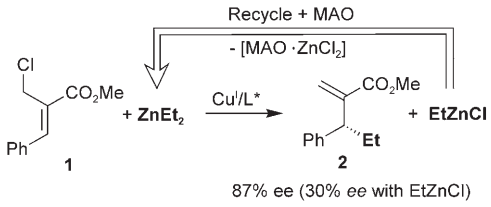

Scheme 1. Asymmetric S_N2' reactions of **1** employing recycling of EtZnCl to avoid the "low *ee*" reaction manifold.

$$2\,RZnX \overset{K<0.002}{\rightleftharpoons} R_2Zn + ZnX_2 \quad (1)$$

$$2\,RZnX + (AlMeO)_n \rightleftharpoons R_2Zn + ZnX_2 \cdot (AlMeO)_n \quad (2)$$

$$RZnX + ZnMe_2 \rightleftharpoons RZnMe + MeZnX \quad (3)$$

Diorganozinc reagents (ZnR_2) are valuable synthons that are more reactive than organozinc halides (RZnX) and undergo transmetalation reactions much more readily.[5] How-

[a] Prof. A. J. Blake, J. Shannon, Dr. J. C. Stephens, Prof. S. Woodward
School of Chemistry, The University of Nottingham
University Park, Nottingham, NG7 2RD (UK)
Fax: (+44) 115-951-3564
E-mail: simon.woodward@nottingham.ac.uk

ever very few diorganozinc species are commercially available (R = Me, Et, *n*Bu, Ph) and new, technically simple, general routes to their preparation are highly desirable. To the best of our knowledge, in contrast to the known magnesium Schlenk processes,[6] no quantitative study of zinc-based Schlenk equilibria has ever appeared in the literature.

Results and Discussion

Promotion of zinc Schlenk equilibria by MAO: The mixture of $(AlMeO)_n$ species known as MAO is a strong halide scavenger and we believed it would act as a "latent Lewis acid"[7] promoting the forward equilibrium given in Equation (1) by sequestering the $ZnCl_2$. This is example of anti-crown behaviour. Anti- and inverse-crown complexes are species in which multiple Lewis acids surround an occluded Lewis base.[8] The term anti-crown is used if the Lewis base has soft, or intermediate hard–soft acid–base (HSAB)[9] character (e.g., Br, I), of which poly-mercury bound species are the best known (e.g., **3**,[10] Scheme 2). If the occluded Lewis base has much harder HSAB character, usually an anionic oxygen donor, then additional HSAB-matched Lewis acids are usually present (e.g., Na, K, Mg as in the inverse-crown species **4**,[11] Scheme 2).

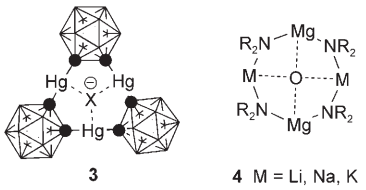

Scheme 2. Representative examples of anti-crown **3** and inverse-crown **4** Lewis acids. The $B_{10}H_{10}C_2$ ligands of **3** are shown schematically.

Ambient temperature ^{13}C NMR studies showed that MAO promotes the zinc Schlenk equilibrium [Eq. (2)] through anti/inverse-crown $ZnCl_2$ behaviour. Stepwise addition of MAO (0.75–3.0 equiv) to solutions of EtZnCl in THF (0.5 M) at 22 °C results in fast exchange of all the ethyl substituents, leading to observation of an averaged $ZnCH_2$ methylene signal in the ^{13}C NMR spectrum (δ_{obs}). As the MAO concentration increases, the value of δ_{obs} increases from $\delta_C = -0.4$ ppm (for pure EtZnCl, δ_X) towards that for pure $ZnEt_2$ $\delta_C = 2.8$ ppm (δ_{R2}) indicating an increased population of $ZnEt_2$ (behaviour shown schematically in Figure 1).

This chemical shift change can be modelled by using Equations (4) and (5) ($[Zn_{tot}]$ and $[Al_{tot}]$ are the total concentration of all zinc and aluminium species present in the system, see Experimental Section). This procedure gives $K = 0.19 \pm 0.05\ M^{-1}$. Putting the K value back into Equation (2) allows the percentage speciation to be determined (Figure 2). At 0.5 M equimolar quantities of EtZnCl and MAO, about 20% of the mixture is converted to $ZnEt_2$. Under identical conditions, no $ZnEt_2$ is spectroscopically detectable in pure 0.5 M EtZnCl (in THF), indicating that Equilibrium (1) is significantly promoted by the presence of MAO. Interestingly, new signals at approximately −13, 8.5 and 9.5 ppm are also present in the EtZnCl/MAO mix: they clearly arise from the anti/inverse-crown co-product MAO–$ZnCl_2$ [Eq. (2)], but the available spectroscopic data does not allow its structure to be determined.

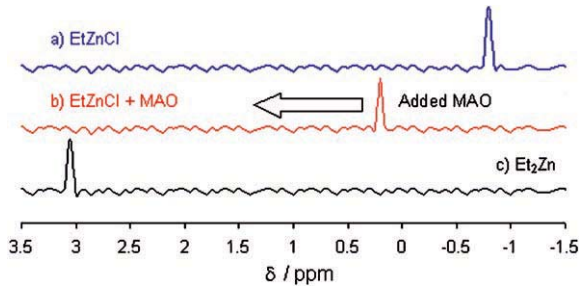

Figure 1. Chemical shift behaviour of the time averaged ^{13}C NMR spectra of the $ZnCH_2$ signal of the species EtZnY (Y = Cl, Et) at 22 °C. a) Pure EtZnCl; b) EtZnY mixtures; c) pure $ZnEt_2$.

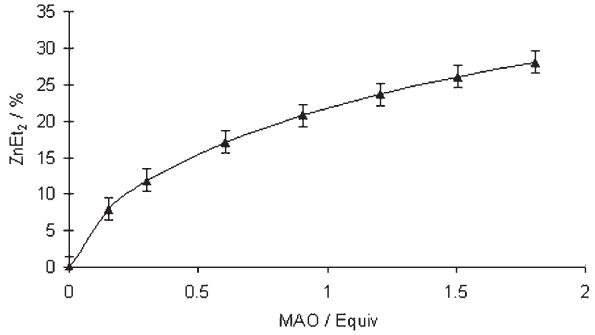

Figure 2. Calculated percentage of $ZnEt_2$ on addition of MAO to a 0.5 M solution of EtZnCl.

$$[ZnR_2] = \frac{[Zn_{tot}]}{2}\left(\frac{\delta_{obs}-\delta_X}{\delta_{R2}-\delta_X}\right) \quad (4)$$

$$K = \frac{[ZnR_2]^2}{([Zn_{tot}]-2[ZnR_2])^2} \cdot \frac{1}{([Al_{tot}]-[ZnR_2])} \quad (5)$$

Despite the clear presence of $ZnEt_2$ in the MAO-promoted EtZnCl [Eq. (2)], the addition of such mixtures to 2-cyclohexenone leads mainly to uncharacterised oligomeric species in THF (Scheme 3) rather than the desired **5a**. In none of the cases was more than a trace amount of the 1,4-methyl addition product detected. Changing the organozinc reagent to the commercially available $PhCH_2ZnBr$ (0.5 M, THF) gave similarly low yields of 3-benzylcyclohexanone **5b** (Table 1, entry 3). Attempted optimisation, varying the temperature (−30, −50 or −65 °C), copper source (library of 11) or added ligands (library of 50) had little effect on the yield of **5b** in THF. In all cases complete conversion was attained within 60 min, but without improvement in the yield of **5b**. The optimal catalyst was found to be copper(I) thiophene-

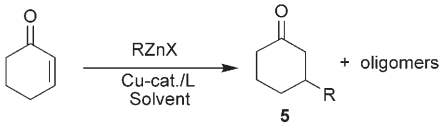

5a R = Et, **5b** R = CH_2Ph, **5c** R = 4-$MePhCH_2$,
5d R = 4-*i*$PrPhCH_2$, **5e** R = 4-$BrPhCH_2$, **5f** R = $EtO_2C(CH_2)_3$

RZnX	Source
A: EtZnCl	$ZnEt_2$ + $ZnCl_2$ in THF
B: $PhCH_2ZnBr$	commercial in THF
C: $PhCH_2ZnBr$	$PhCH_2Br$ + Zn in DME
D: $ArCH_2ZnBr$	$ArCH_2Br$ + Zn in DME
E: $EtO_2C(CH_2)_3ZnBr$	commercial, THF removed and replaced by DME

Scheme 3. Organozinc addition to 2-cyclohexenone (in *D*, Ar = 4-Me, 4-*i*Pr, 4-Br).

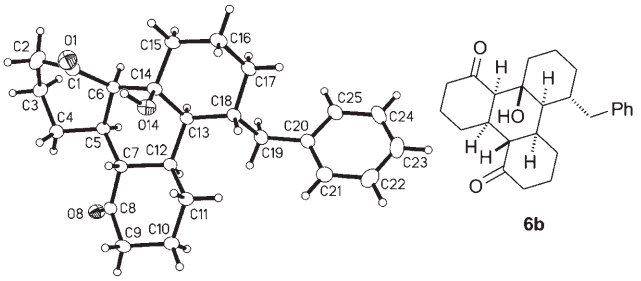

Figure 3. Molecular structure and numbering scheme for tetracyclic oligomer **6**.

Table 1. MAO-promoted RZnX reactions with 2-cyclohexenone.[a]

Run	RZnX Source [equiv]	Solvent	*T* [°C]	Ligand [4 mol%]	MAO [equiv][b]	1,4-Yield [%] [c]	Oligomers [%][d]	**6** [%][c]
1	none	THF	−30	$P(OPh)_3$	5	0[e]	63	–
2	**B** $PhCH_2ZnBr$ (2.8)	THF	−30	$P(OPh)_3$	0	0[e] (**5b**)	39	–
3	**B** $PhCH_2ZnBr$ (2.8)	THF	−30	$P(OPh)_3$	5	16[e] (**5b**)	80	–
4	**B** $PhCH_2ZnBr$ (2.8)	THF	−65	$P(OPh)_3$	5	8[e] (**5b**)	68	–
5	**B** $PhCH_2ZnBr$ (0.33)	THF	−30	–	3	n.d.[f]	n.d.	20–25 (**6b**)
6	**C** $PhCH_2ZnBr$ (2.0)	DME	−30	$P(OPh)_3$	6	53[e] (**5b**)	43	–
7	**C** $PhCH_2ZnBr$ (2.0)	DME	−30	–	3	53 (**5b**)	n.d.	–
8	**C** $PhCH_2ZnBr$ (2.0)	DME	−30	–	6	70 (**5b**)	n.d.	–
9	**D** 4-$MePhCH_2ZnBr$ (2.0)	DME	−30	–	6	60 (**5c**)	n.d.	–
10	**D** 4-*i*$PrPhCH_2ZnBr$ (2.0)	DME	−30	–	6	70 (**5d**)	n.d.	–
11	**D** 4-$BrPhCH_2ZnBr$ (2.0)	DME	−30	–	6	72 (**5e**)	n.d.	–
12	**E** EtO_2C-$(CH_2)_3ZnBr$ (2.0)	DME	−30	–	6	20 (**5f**)	n.d.	10 (**6f**)

[a] Standard conditions: [Cu(TC)]/RZnBr/cyclohexenone: 0.01:4:2.0 mmol; DME (or THF)/toluene 3:4 v/v; total volume DME or THF (12 mL); total volume toluene (including that added with any MAO, 16 mL); 1 h reaction time. [b] Added as toluene solution (10 wt.%, AlMeO). [c] Isolated yield after chromatography unless otherwise indicated. [d] Estimated from reaction mass balance. [e] Determined by GC on a BP20 column using a tridecane internal standard (25 μL). [f] Not determined.

carboxylate[13] [Cu(TC)] (2 mol%) at −30 °C by using either no ligand or $P(OPh)_3$ (4 mol%). Due to this initial resistance to optimisation, attempts were made to identify the nature of the oligomeric species formed in these reactions. Fortunately, the major oligomeric product derived from $PhCH_2ZnBr$ could be crystallised and X-ray studies revealed the tetracycle **6b** (R = CH_2Ph) (Figure 3). Remarkably, **6b** is isolated as a single diastereoisomer (in 20–25% yield) resulting from three consecutive conjugate additions and a 1,2-addition termination step, generating seven contiguous stereocentres. The cascade in Scheme 4 is a probable explanation of its origin. Reinvestigation of the EtZnCl/MAO/cyclohexenone mixtures by mass spectrometry revealed the presence of the ethyl analogue **6a** in the oligomeric mixture; however, this could not be isolated as a pure crystalline solid.

In poorly chemoselective catalytic 1,4-additions of organometallics, capture of the initial (kinetic) enolate by additional enone starting material is known to be a significant competition pathway. Mixed diastereomers of the derived so-called "dimer"[14] products (i.e., those formed by protonation of the enolate structure within **7**, Scheme 4) are commonly seen as high-boiling impurities in the gas chromatography (GC) traces of 2-cyclohexenone derived reaction mixtures. Nevertheless, the formation of tetracyclic trimer products, such as **6**, does not seem to have been noted previously. Such behaviour is rare, but could be described as a MIMIMIRC process (MI = Michael; RC = Ring Closing) using the nomenclature of Posner.[15] Traces of a related product, derived from 1-

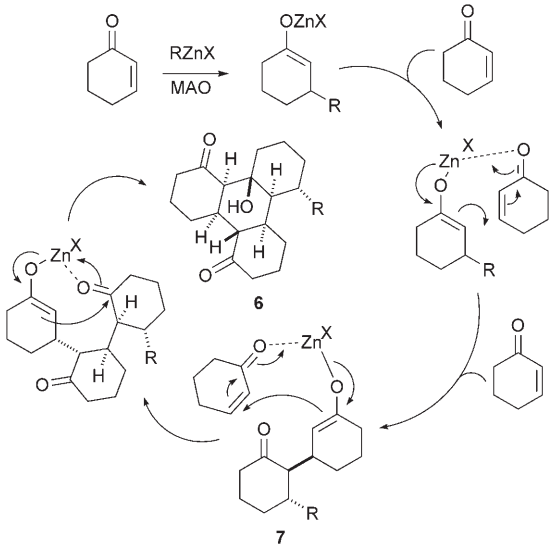

Scheme 4. Proposed mechanism for the formation of **6** (R = CH_2Ph).

cyanocyclohexene, have been claimed,[16] but in this case no supporting evidence was presented. In our original MAO-promoted S_N2' $ZnEt_2$ additions to the allylic chloride **1** (Scheme 1), the choice of solvent dramatically affected both the yield and stereoselectivity, both being favoured by the use of dimethoxyethane (DME). We believed that this solvent might also stabilise the initial kinetic enolates, preventing the cascade reaction leading to **6**. Therefore, solutions of $ArCH_2ZnBr$ in DME were prepared by direct, and very clean, insertion of zinc into the C–Br bond of $ArCH_2Br$. Use of DME for the formation of RZnI species was first reported by Zakharin and Okhlobystin,[17] but this approach has been rarely used, despite the fact that the higher boiling point of DME (85 °C) is beneficial to the insertion rate. Indeed, DME as solvent, in the absence of any added ligand, allows synthetically useful yields of the conjugate-addition products **5a–f** to be realised (Table 1, entries 6–10), presumably due to increased stability of the initial enolates. However, use of other polyether or donor solvents was not as profitable (diglyme, triglyme and DMF gave 5–37% yield of **5b**). The $PhCH_2ZnBr$/MAO procedure is much more effective than use of pure $Zn(CH_2Ph)_2$ (the latter gave $<20\%$ conversion under the conditions investigated), and appears to be one of the best methods for 1,4-benzylic addition. One functionalised organozinc ester $BrZn(CH_2)_3CO_2Et$ could be added to 2-cyclohexenone in poor yield (Table 1, entry 12). However, in this case a significant side product was the derived cascade oligomer **6f**, which could be isolated (10%). The formation of **6f** was favoured by the residual THF present in the commercial organometallic used. Attempts to carry out the copper-catalysed reaction of 2-cyclohexenone and $PhCH_2ZnBr$ by using only 0.75 equivalents of MAO were unsuccessful, producing only traces of the addition product **5b** (4%). In fact, the yield of the MAO-promoted reaction of $PhCH_2ZnBr$ and 2-cyclohexenone clearly demonstrates saturation behaviour (Figure 4) with respect to the MAO concentration.

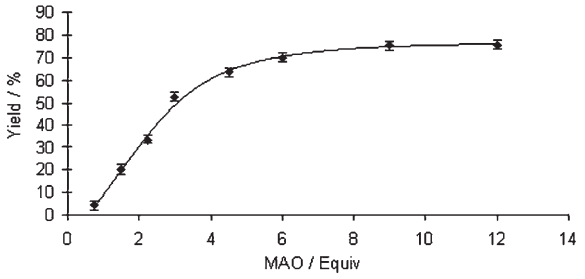

Figure 4. Yield of 1,4-addition product **5b** against MAO present in reaction mixture for the reaction of 2-cyclohexenone with $PhCH_2ZnBr$.

If equilibrium in Equation (2) is the only process in which MAO participates, then the observed yield of **5b** estimates the quantity of $Zn(CH_2Ph)_2$ present in the reaction mixture (as only this traps onto 2-cyclohexenone). As long as the DME solvent minimises the quantity of oligomers formed, then the approximation that $[Zn(CH_2Ph)_2] \approx [\mathbf{5b}]$ will be valid and K can be estimated by using Equation (5). Under these conditions, a plot of $[CA_{obs}]^2/([Zn_{tot}]-2[CA_{obs}])^2$ against $([Al_{tot}]-[CA_{obs}])$ is expected to be a straight line of gradient K; here $[Zn_{tot}]$ and $[Al_{tot}]$ are again the total concentration of all zinc and aluminium species present in the system at a given composition, and $[CA_{obs}]$ is the measured concentration of **5b** based on its GC yield. The derived plot of Equation (5) was found to be linear (correlated coefficient = 0.995) for 1.5–9.0 equivalents of MAO to $PhCH_2ZnBr$ and gives $K = 4.8 \pm 0.8\,\text{M}^{-1}$. This value is significantly higher than the $K = 0.19\,\text{M}^{-1}$ determined from the NMR experiments conducted on EtZnCl/MAO. Such behaviour cannot be caused by under estimating the $[Zn(CH_2Ph)_2]$ by equating this to [**5b**] (i.e., not allowing for a minor oligomerisation component). Equation (5) leads to an overestimation of K, as the concentration of MAO found in the reaction mixture is less than expected. The kinetic enolate formed from the conjugate addition to 2-cyclohexenone is a potent Lewis base and competitively binds MAO in the reaction mixture (K_2, Scheme 5). Such behaviour lowers the

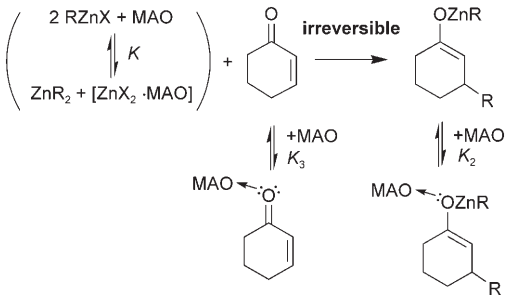

Scheme 5. Competitive MAO binding by both the kinetic enolate product and the starting 2-cyclohexenone.

effective concentration of MAO available to promote the zinc Schlenk equilibrium [Eq. (2)] and leads to the overestimation of K when Equation (5) us used. A similar, but less effective, MAO competitive binding to 2-cyclohexenone also exists (K_3, Scheme 5). It will also be seen that the reaction sequence in Scheme 5 prevents Le Chatelier's principle from operating as although irreversible enolate formation should drive the equilibrium in Equation (2) to completion (through ZnR_2 removal), this is self-limited. Generation of the enolate product also removes MAO (through K_2), lowering the MAO concentration available to promote the initial zinc Schlenk process [Eq. (2)].

Although it is clear that the reaction sequences in Scheme 5 will account for Equation (5) over reporting the value of K, deconvolution of the additional equilibrium constants K_2 and K_3 could not be attained. ^{13}C NMR studies of solutions of MAO and 2-cyclohexenone in THF at low temperatures are not possible due to the presence of multiple broad signals arising from the presence of a mixture of quadrupolar aluminium MAO species (^{27}Al, $I = 5/2$). Under fast exchange conditions at ambient temperature, K_3 could

not be independently measured due to competing 2-cyclohexenone polymerisation and some formation of the methyl analogue of **6**. Similarly, K_2 could not be independently measured at low temperature due to broad signals; attempted quantification at ambient temperature led to decomposition only. As an additional complication, the literature preparative routes[18] to $Zn(CH_2Ph)_2$ (required to form the enolate in Scheme 5) lead to impure samples containing a second species, which could be characterised as $PhCH_2ZnCl$. By using an Et_2O solvent rather than 1,4-dioxane the formation of pure $Zn(CH_2Ph)_2$ was achieved. There is significant binding of the added MAO by the kinetic enolate product formed by the conjugate addition; therefore, it is necessary to use a significant excess of MAO in the chemistry of Scheme 3. An attempted in situ quench of the kinetic enolate, in which TMSCl, or BEt_3 was added to prevent it from binding to MAO, had no effect on the reaction.

Promotion of zinc Schlenk equilibria by other added ZnR_2 species: In a seminal 1971 paper, Evans and co-workers reported ^{1}H NMR studies of ethyl exchange between $ZnEt_2$ and EtZnCl.[2] We extended these investigations by using ^{13}C NMR spectroscopy, as it was anticipated this would provide better spectral separation in the subsequent more complicated reaction mixtures. A combination of $ZnEt_2$ (0.25 M) and $ZnCl_2$ (0.15 M) in THF led to clean formation of EtZnCl (0.3 M) containing residual $ZnEt_2$ (0.1 M); no other appreciable species were detected. The complimentary ^{1}H NMR integrals of the sample are consistent with the complete formation of EtZnCl, in which there is a very low K value for the equilibrium in Equation (1). Variable-temperature (VT) studies (+22 to −100 °C) confirmed exchange with the free $ZnEt_2$, and a coalescence temperature of −45 °C (Figure 5). We propose that this exchange takes place through the transient intermediate [EtZn(μ-Cl)(μ-Et)ZnEt] **8**.

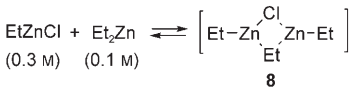

8

Relevant ^{13}C NMR signals from this system are summarised in Table 2 along with the organozinc species studied in this investigation for comparison. A mixture of EtZnCl (0.26 M) and $ZnMe_2$ (0.26 M) results in little apparent reaction at ambient temperature; signals assignable to both the EtZnCl ($\delta_C = 2.8$, 12.5 ppm) and $ZnMe_2$ ($\delta_C = 10.2$ ppm) are present. However, cooling the mixture reveals a fluxional process leading to the observation (at −100 °C) of eight sig-

Table 2. ^{13}C NMR shifts [ppm] for the species RZnY species (R = Me, Et; Y = Cl, Me, Et).

Species	Solvent	T [°C]	c [M]	Signals [ppm] (assignment)
$ZnEt_2$	THF	22	0.25	12.5 (Me), 2.8 (CH_2)
$ZnMe_2$	THF/toluene[a]	22	0.26	−10.2 (Me),
EtZnCl	THF	22	0.3	13.2 (Me), −0.4 (CH_2)
EtZnCl	THF	−100	0.3	13.9 (Me), −0.6 (CH_2)
EtZnMe	THF/toluene[a]	−100	0.26[b]	14.0 (CH_2*Me*), 3.1 (*CH_2*Me), −11.1 (ZnMe)
MeZnCl	THF/toluene[a]	−100	0.26[b]	−14.8 (ZnMe)

[a] 13% toluene v/v in THF. [b] Total concentration of all Zn species present.

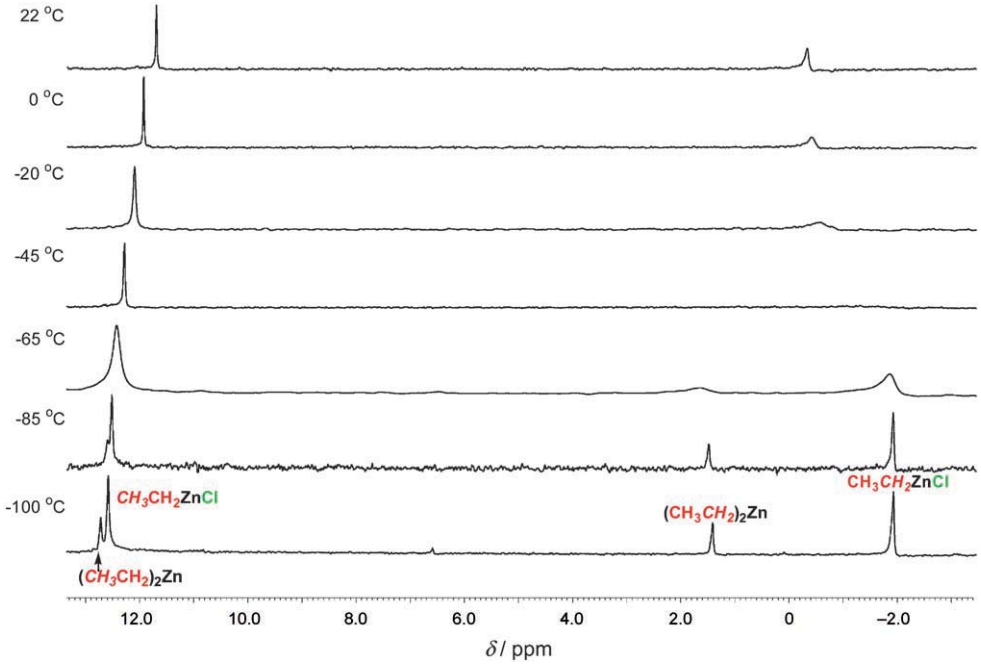

Figure 5. Variable-temperature partial ^{13}C NMR spectra of EtZnCl in the presence of $ZnEt_2$.

nals, one of trace and batch dependent intensity (see footnote of Figure 6). Based on the data of Table 1 we assign this behaviour to scrambling of all of the zinc substituents (Scheme 1) via the 4-membered transition state **9**.

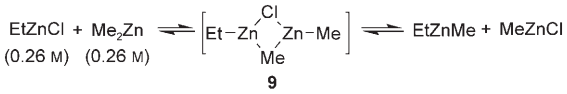

9

The trace and variable signal at $\delta_C = 2.8$ ppm is assigned to very small amounts of $ZnEt_2$ (generated by a second round of Schlenk redistribution between EtZnMe and EtZnCl). Comparison of the ^{13}C NMR data of the four major zinc species indicates that their ratio is essentially 1:1:1:1, implying a K value of ≈ 1 for Equation (6) (R = Et, $[Zn_{tot}] = 0.26$ M). Although the equilibrium in Equation (3) has previously been investigated by calorimetry,[19] this is the first confirmation of the formation of mixed diorganozinc species by NMR spectroscopy.

$$K = \frac{[EtZnMe][MeZnCl]}{[EtZnCl][ZnMe_2]} \approx 1 \qquad (6)$$

As both RZnCl (R = Me, Et) species are relatively unreactive, we believed it would be possible to selectively utilise EtZnMe alone in subsequent catalytic reactions. Further, as Zn–Me bonds are among the strongest in organozinc chemistry ($D^0 \approx 68$ kcal mol^{-1}), selective transfer of only "Et" should also be viable, demonstrating the use of methyl as a "non-transferable group".[20] The utility of EtZnMe, generated in these NMR procedures, is confirmed by its interaction with 2-cyclohexenone in the presence of $Cu(OTf)_2$ and Feringa's phosphoramidite (**10**)[21] (Table 3). Modification of the solvent mixture results in >90% *ee* values and minimal methyl transfer, consistent with the presence of EtZnMe. Control reactions including EtZnCl give negligible yields of conjugate addition product as expected.

Although the transfer of "Et" could be readily attained, attempts to promote other "R" groups to transfer from the RZnMe species were complicated by a competing "Me" transfer to the enone. For example, BuZnMe was readily prepared from BuZnCl and $ZnMe_2$, but only 16–23% yield

Table 3. Asymmetric addition of EtZnCl to 2-cyclohexenone under promoted equilibrium conditions.[a]

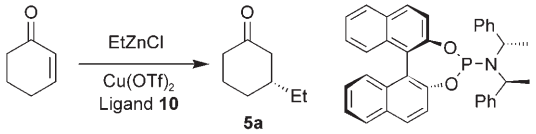

5a **10**

EtZnCl/$ZnMe_2$	THF/toluene	Yield **5a**/%[b]	*ee*/%[b]
1:0	2:1	<2	<2
1:3	2:1	5	26
1:0	1:9	4	<2
1:3	1:9	80	83
1:1	2:98	67	85
1:3	2:98	60	92

[a] EtZnCl prepared from $ZnCl_2$ and neat $ZnEt_2$. Addition to 2-cyclohexenone (0.5 mmol) with $Cu(OTf)_2$ (2 mol%) and (*R,S,S*)-**10** (4 mol%) in 3.9 mL of the solvent mix: THF/toluene; −30 °C, 1 h. [b] Determined by GC on a Lipodex-A column using nonane as an internal standard (25 μL) for yield calculations; (*R*)-product observed in all cases.

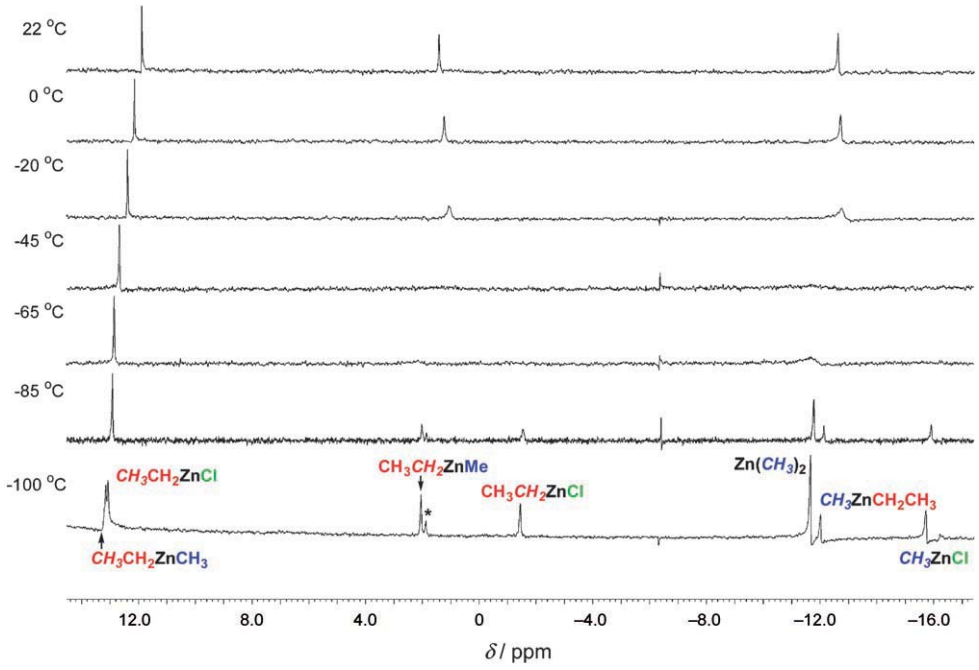

Figure 6. Variable-temperature ^{13}C NMR spectra of EtZnCl in the presence of $ZnMe_2$. The species marked "*" is assigned to the CH_2 group of $ZnEt_2$ generated in small quantities through secondary disproportionation of EtZnMe.

of the butyl 1,4-addition product was realised under the conditions of Table 3. The mass balance of these reactions has found to be the equivalent 1,4-methyl addition product (4–20%) and unreacted 2-cyclohexenone. Attempts to use "$TMSCH_2$" as an alternative non-transferable group by reacting BuZnCl and $Zn(CH_2TMS)_2$ produced a mixed diorganozinc species of very low reactivity. It could be concluded, at present, that the best approach to using promoted zinc Schlenk equilibria is to use the MAO procedure given above.

Conclusion

^{13}C NMR studies have demonstrated explicitly that the Lewis acids $ZnMe_2$ and MAO cause disproportionation of RZnX reagents into RZnMe and ZnR_2 respectively. The promoted equilibria favour the formation of diorganozinc species by at least two orders of magnitude more than the unpromoted case [Eq. (1)]. Modelling of both the NMR data and chemical quenching data are both in accord with the equilibria in Equations (2) and (3) and showed K values from 0.2 to 4.5 M^{-1}. Significant populations of RZnMe or ZnR_2 are achieved and these can be used in 1,4-conjugate addition chemistry. However, the resulting kinetic enolate can also participate in competing Michael additions to the starting enone, resulting in previously uncharacterised cascade products. Using excess MAO can overcome this problem as the enolate is captured by the MAO. This approach is presently preferable to forming mixed $RZn(R_{NT})$ species (R_{NT} = non-transferable group). Although the latter species are easily prepared and characterised by ^{13}C NMR spectroscopy, further investigation is needed to attain chemospecific 1,4-addition of just "R" from $RZn(R_{NT})$ species. This is currently underway.

Experimental Section

General: All experiments were carried out under an argon atmosphere by using standard Schlenk techniques. Solvents were distilled from suitable drying agents prior to use: THF and DME from sodium/benzophenone, 2-cyclohexenone was distilled and stored under argon. ^1H and ^{13}C NMR spectra were recorded by using either a Bruker AM400 or a JEOL EX270 spectrometer, details of the NMR monitoring experiments are given below. For all samples, δ values were referenced to residual solvent peaks. All J values are in Hz. Infrared spectra were recorded by using a Perkin Elmer 1600 Series FTIR machine. Mass spectra were recorded by using electron ionisation (EI) or chemical ionisation (CH_4, CI) techniques using a Micromass 70E machine. GC analyses was performed by using a Varian 3380 gas chromatograph through a Lipodex A or BP20 column, from which the yield was determined by using an appropriately calibrated internal standard. TLC was performed on Merck Silicagel 60 $F_{254+366}$ precoated plates (0.25 mm) silica. The plates were visualised by the use of a combination of ultraviolet light (254 and 366 nm) and/or aqueous potassium permanganate or anisaldehyde and then heat. Liquid chromatography was by forced flow (flash chromatography) including the solvent systems indicated by using silica gel 60 (220–240 mesh) supplied by Fluka. The compound [Cu(TC)] was prepared by a literature method,[13] all other compounds were commercial products, specifically: $ZnMe_2$ (2.0 M toluene solution; Aldrich), $ZnEt_2$ (neat 98%; Strem), MAO (10% w/w in toluene; Aldrich).

NMR investigations: NMR studies were carried out on a JEOL-270 MHz spectrometer (270.2 MHz for ^1H; 67.9 MHz for ^{13}C) at temperatures between −100 °C and RT. Studies were conducted in undeuterated THF dried by distillation from sodium/benzophenone. Peak shape optimisation was attained by manual optimisation of the repeated FID shape and area. All NMR scales were referenced to the lower frequency signal of THF (δ_H = 1.80 ppm; δ_C = 26.7 ppm). All preparations were carried out under argon using flame-dried glassware. Key ^{13}C NMR shifts are reported in Table 2. The systems were allowed to equilibrate for 0.25–16 h at RT, but in all cases identical results were attained irrespective of the incubation period.

NMR studies of EtZnCl: Ethyl exchange between $ZnEt_2$ and EtZnCl was characterised by using VT ^{13}C NMR spectroscopy. Fused $ZnCl_2$ (102 mg, 0.75 mmol) was suspended in THF (5.0 mL) and neat $ZnEt_2$ (48 μL, 92 mg, 0.75 mmol) and the mixture equilibrated at RT (16 h). A sample (0.7 mL, 0.3 M in EtZnCl) was transferred by syringe to a flame-dried NMR tube under argon. An equivalent sample containing excess $ZnEt_2$ was prepared by addition of $ZnEt_2$ (80 μL, 154 mg, 1.25 mmol) to fused $ZnCl_2$ (102 mg, 0.75 mmol) and THF (5.0 mL), leading to a sample that contained, nominally, EtZnCl (0.3 M) and $ZnEt_2$ (0.1 M). The VT ^{13}C NMR spectra of this mixture are shown in Figure 5. At −85 °C the ratio of ^1H NMR methylene integrals for EtZnCl:$ZnEt_2$ were 1.50–1.58 [a value of 1.50 is expected for K = 0 in Equation (1)]. The system reached coalescence at −45 °C.

NMR studies of the reaction of EtZnCl with $ZnMe_2$: A nominal solution of EtZnCl (1.50 mmol, 0.3 M) was prepared from the reaction of neat $ZnEt_2$ (48 μL, 92 mg, 0.75 mmol) to fused $ZnCl_2$ (102 mg, 0.75 mmol) in THF (5.0 mL). The equilibrated EtZnCl solution was treated at RT with $ZnMe_2$ (0.75 mL, 1.50 mmol, 2.0 M, toluene) and the mixture stirred at RT (16 h). A sample (0.7 mL) was transferred to a flame-dried NMR tube under argon that nominally contained EtZnCl (0.26 M) and $ZnMe_2$ (0.26 M) in a 13:87 v/v mixture of toluene/THF. The VT ^{13}C NMR behaviour of this sample is shown in Figure 6.

NMR studies of the reaction of EtZnCl with MAO: Direct NMR analysis of mixtures of organozinc species and MAO $(AlMeO)_n$ solutions are complicated by the oligomeric nature of the MAO and the quadrupole nature of the aluminium nucleus (^{27}Al, 100%, I = 5/2). Below −10 °C overlapped broad signals were observed (^1H NMR studies) or the presence of multiple signals (^{13}C NMR studies). We believe the latter is due to zinc species interacting with the differing MAO oligomers. Fast exchange conditions at RT or 0 °C were therefore employed. A nominal 1.25 M solution of EtZnCl (25.0 mmol) was prepared from the reaction of neat $ZnEt_2$ (1.28 mL, 12.50 mmol) to fused $ZnCl_2$ (1.7 g, 12.50 mmol) in THF (18.7 mL), and the resulting solution was stirred at RT (1 h). After this time, 2 mL of the solution was transferred into a second flame-dried Schlenk and MAO (0.25–3.00 mL, 10% w/w in toluene, ~0.38–4.52 mmol of "AlMeO") was added, followed by toluene such that the total volume of toluene added was consistently 3.0 mL. The mixture was then stirred at RT (15 min). A sample (0.7 mL) was then transferred to a flame-dried NMR tube under argon that nominally contained 0.5 M total zinc species and 0.076–0.90 M total aluminium species in a 3:2 v/v mixture of toluene/THF. Equivalent runs at 22 °C and with greater amounts of MAO (up to 3.0 equiv) produced similar spectra (not shown) except that the final chemical shift of the $Zn(CH_2)_{ave}$ was greater (from −0.4–2.2 ppm). The value K was determined for added MAO concentrations of up to 0.9 M through Equations (4) and (5). A plot of Equation (5) (using $[ZnR]_2$ (R = Et) attained from Equation (4) using the crude NMR data) gave $K = 0.19 \pm 0.05$ (correlation coefficient 0.986).

Preparation of EtZnCl on a synthetic scale: To a dried Schlenk tube under an argon atmosphere containing $ZnCl_2$ (0.95 g, 7.0 mmol) dried THF (12.3 mL) was added. The solution was stirred for 10 min and then neat Et_2Zn (0.72 mL, 7.0 mmol) was added dropwise. The resulting cloudy solution was stirred for 1 h and then the THF was removed under high vacuum. The resulting white solid was then dissolved in the desired solvent system and stirred for 20 min to give a 1.07 M solution.

Preparation of EtZnMe from EtZnCl and Me_2Zn on a synthetic scale: To a dried Schlenk tube under an argon atmosphere was added EtZnCl (1.95 mL, 2.1 mmol) followed by dropwise addition of Me_2Zn (2 M toluene solution). The resulting cloudy solution was stirred for 30 min and then diluted if necessary to give a 0.41 M solution.

General procedure for the 1,4-addition of EtZnMe to 2-cyclohexenone, preparation of 5a: A dried Schlenk tube was charged with $Cu(OTf)_2$ (3.62 mg, 0.01 mmol) and (*R*,*S*,*S*)-**10** (10.79 mg, 0.02 mmol). Dry solvent (0.3 mL) was introduced, the stirred mixture cooled to −30 °C and stirred for 30 min before EtZnMe (0.41 M) was added. The resulting solution was stirred for a further 30 min and 2-cyclohexenone (48.5 μL, 0.5 mmol) was added dropwise. Stirring was continued for 1 h at −30 °C, then the reaction was quenched by cautious addition of aqueous HCl (2 mL, 2 M). Nonane (25 μL) was added and the organic layer was passed through a plug of silica and the yield determined by quantitative GC analysis. (*R*)-3-Ethylcyclohexanone (**5a**) was attained, 60 % (92 % *ee*). Colourless oil; ^{1}H NMR (400 MHz, $CDCl_3$, 25 °C): δ_H = 2.48–2.25 (m, 3H), 2.11–1.92 (m, 3H), 1.79–1.62 (m, 2H), 1.49–1.29 (m, 3H), 0.94 ppm (t, *J* = 7.6, 3H; CH_2*Me*); ^{13}C NMR (100 MHz, $CDCl_3$): δ_C = 212.2, 47.9, 41.5, 40.6, 30.9, 29.3, 25.3, 11.2 ppm. These data are concordant with published values and the spectrum identical to an authentic sample.[21] The enantiomeric excesses were determined by chiral GC (Lipodex A, isothermal 75 °C): (*R*)-**2** 9.9 min; (*S*)-**2** 10.2 min.

Preparation of $ArCH_2ZnBr$ in DME: A dried Schlenk tube was charged with granular zinc powder (1.83 g, 28.0 mmol; Acros, 200 mesh, 99.9999 % purity), heated under vacuum with a hot-air gun and backfilled with argon. The evacuation/heating procedure was repeated three times. Anhydrous DME (26.3 mL) and TMSCl (71 μL, 0.56 mmol) were introduced and the mixture stirred vigorously at RT (30 min). The mixture was cooled to 0 °C and the appropriate benzylic bromide (14.0 mmol) added dropwise. The mixture was stirred at RT until no starting bromide was present by TLC (1 h). Stirring was stopped and the supernatant $ArCH_2ZnBr$ solution (0.5 M in DME) removed by syringe once the excess zinc powder had settled. Equivalent preparations in THF were readily attained.

General procedure for 1,4-addition of $ArCH_2ZnBr$ to 2-cyclohexenone (leading to 5b–f): A dried Schlenk tube was charged with [Cu(TC)] (7.6 mg, 0.01 mmol) and dry DME (4.0 mL). The stirred mixture was cooled to −30 °C and MAO (10 wt % in toluene, 6.0–24.0 mmol, 3–12 equiv) added followed by toluene such that the total volume of toluene added remained 16.0 mL. The yellow reaction mixture was stirred for 10 min at −30 °C after which RZnBr (8.0 mL, 0.5 M, DME, 4.0 mmol) was added followed by 2-cyclohexenone (194 μL, 2.0 mmol). Stirring was continued for 1 h at −30 °C after which time the reaction was quenched by cautious addition of aqueous HCl (8 mL, 2 M). The reaction mixture was extracted with Et_2O (2 × 25 mL), the organic phase was washed with water (25 mL) and brine (25 mL), and dried ($MgSO_4$) and the solvent evaporated. The product was isolated by flash chromatography using light petroleum (b.p. 40–60 °C)/Et_2O (7:1 or 5:1).

Alternatively for the purpose of GC analysis, the same reaction was carried out using 2-cyclohexenone on a 0.5 mmol scale. The reaction mixture was quenched as above, followed by the addition of tridecane ($C_{13}H_{28}$) (25 μL). The organic layer was passed through a plug of silica and then analysed by GC. Isolated yields were within 5 % of those determined by GC.

3-Benzylcyclohexanone (5b, R = CH_2Ph): Yield 271.1 mg (72 %); ^{1}H NMR (400 MHz, $CDCl_3$, 25 °C): δ_H = 7.26–7.14 (m, 5H; Ar), 2.64–2.58 (m, 2H; CH_2Ar), 2.41–2.00 (m, 6H), 1.86–1.78 (m, 1H), 1.62–1.55 (m, 1H), 1.42–1.35 ppm (m, 1H); ^{13}C NMR (100 MHz, $CDCl_3$): δ_C = 211.7, 139.4, 129.1 (d), 128.4 (d), 126.2, 47.9, 43.0, 41.4, 41.0, 30.9, 25.1 ppm; HRMS (EI): calcd for $C_{13}H_{16}ONa^+$: 211.1099; found: 211.1105 $[M+Na]^+$; GC (BP20, initial temperature 120 °C for 15 min, then ramp 20 °C min^{-1} to 180 °C) retention time 29.8 min. These data are concordant with published values.[22]

3-[(4-Tolyl)methyl]cyclohexanone (5c, R = $CH_2C_6H_4Me$-4): Yield 242.2 mg (60 %). ^{1}H NMR (400 MHz, $CDCl_3$, 25 °C): δ_H = 7.11 (d, *J* = 8.9, 2H; Ar), 7.03 (d, *J* = 8.9, 2H; Ar), 2.60 (d, *J* = 6.8, 2H; CH_2), 2.34 (s, 3H; Me), 2.42–2.26 (m, 3H), 2.11–2.02 (m, 3H), 1.92–1.88 (m, 1H), 1.70–1.64 (m, 1H), 1.48–1.42 ppm (m, 1H); ^{13}C NMR (100 MHz, $CDCl_3$): δ_C = 211.7, 136.3, 135.7, 129.1 (d), 129.0 (d), 47.9, 42.5, 41.4, 41.0, 30.9, 25.1, 21.0 ppm; IR ($CHCl_3$): $\tilde{\nu}$ = 2926, 2863, 1706, 1603, 1448, 1347, 1314 cm^{-1}; HRMS (EI): calcd for $C_{14}H_{18}ONa^+$, 225.1255; found: 225.1236 $[M+Na]^+$.

3-[(4-Isopropylphenyl)methyl]cyclohexanone (5d, R = $CH_2C_6H_4i$Pr-4): Yield 322.5 mg (70 %). ^{1}H NMR (400 MHz, $CDCl_3$, 25 °C): δ_H = 7.14 (d, *J* = 8.0, 2H; Ar), 7.04 (d, *J* = 8.0, 2H; Ar), 2.88 (sept, *J* = 6.9, 1H; C*H*-(CH_3)), 2.60 (ABX, *J* = 13.6, 6.5, 2H; CH_2Ar), 2.40–2.20 (m, 3H), 2.09–2.01 (m, 3H), 1.93–1.82 (m, 1H) 1.68–1.55 (m, 1H), 1.42–1.36 (m, 1H), 1.24 ppm (d, *J* = 6.9, 6H; $2CH_3$); ^{13}C NMR (100 MHz, $CDCl_3$): δ_C = 211.8, 146.7, 136.7, 129.0 (d), 126.4 (d), 47.8, 42.6, 41.5, 41.0, 33.7, 31.0, 25.2, 24.1 ppm (d); IR ($CHCl_3$): $\tilde{\nu}$ = 2961, 2928, 2871, 1705, 1510, 1449, 1347, 1314, 1055 cm^{-1}; HRMS (EI): calcd for $C_{16}H_{22}ONa^+$: 253.1568; found: 253.1564 $[M+Na]^+$.

3-[(4-Bromophenyl)methyl]cyclohexanone (5e, R = $CH_2C_6H_4Br$-4): Yield 329.0 mg (62 %). ^{1}H NMR (400 MHz, $CDCl_3$, 25 °C): δ_H = 7.41–7.37 (m, 2H; Ar), 7.00–6.97 (m, 2H; Ar), 2.61–2.52 (m, 2H; CH_2Ar), 2.37–2.31 (m, 2H), 2.27–2.20 (m, 1H), 2.06–1.98 (m, 3H), 1.87–1.82 (m, 1H) 1.66–1.55 (m, 1H), 1.37–1.33 ppm (m, 1H); ^{13}C NMR (100 MHz, $CDCl_3$): δ_C = 211.1, 138.3, 131.4 (d), 130.7 (d), 120.0, 47.7, 42.2, 41.3, 40.6, 30.7, 24.9 ppm; IR ($CHCl_3$): $\tilde{\nu}$ = 2931, 2870, 1707, 1592, 1488, 1347, 1314, 1073, 1012 cm^{-1}; HRMS (EI): calcd for $C_{13}H_{15}BrO$: 266.0306; found: 266.0304 $[M]^+$.

Ethyl-4-(3-oxocyclohexyl)butanoate (5f, R = $(CH_2)_3CO_2Et$): ^{1}H NMR (400 MHz, $CDCl_3$, 25 °C): δ_H = 4.09 (q, *J* = 7.2, 2H), 2.44–2.18 (m, 3H), 2.25 (t, *J* = 7.6, 2H), 2.04–1.95 (m, 2H), 1.92–1.55 (m, 5H), 1.39–1.25 (m, 3H), 1.22 ppm (t, *J* = 7.2, 3H); ^{13}C NMR (100 MHz, $CDCl_3$): δ_C = 211.8, 173.5, 60.3, 48.0, 41.5, 38.8, 36.0, 34.3, 31.1, 25.2, 22.1, 14.3 ppm; HRMS (EI): calcd for $C_{12}H_{20}O_3^+$: 212.1412; found: 212.1407 $[M]^+$. These data are concordant with published values.[23]

Representative preparation of tetracycle 6b: A dried Schlenk tube was charged with [Cu(TC)] (7.6 mg, 0.01 mmol) and dry THF (4.0 mL). The stirred mixture was cooled to −30 °C and MAO (10 wt % in toluene, 6 mmol, 6 mL) added. The yellow reaction mixture was stirred for 10 min at −30 °C after which BnZnBr (1.3 mL, 0.5 M, THF, 0.65 mmol) was added *followed by* 2-cyclohexenone (194 μL, 2.0 mmol). Stirring was continued for 1 h at −30 °C and the reaction was then quenched by cautious addition of aqueous HCl (8 mL, 2 M). The reaction mixture was extracted with dichloromethane (2 × 30 mL), the organic phase was washed with water (25 mL), brine (25 mL), dried ($MgSO_4$) and the solvent evaporated. The product was isolated by flash chromatography using light petroleum (b.p. 40–60 °C)/Et_2O (3:1) (R_f = 0.20) then recrystallised using dichloromethane/hexane 58.5 mg (24 %). Positional assignments use the nomenclature of Figure 3. *Geminal*, *anti*, *syn*, *gauche* and long-range couplings are indicated ^{gem}J, ^{anti}J, ^{syn}J , ^{gau}J and $^{1,4}J$ respectively. ^{1}H NMR (400 MHz, $CDCl_3$, 25 °C): δ_H = 7.28 (app. t, *J* = 7.3, 2H; Ph_m), 7.20 (app. t, *J* = 7.3, 1H; Ph_p), 7.16 (app. d, *J* = 7.3, 2H; Ph_o), 4.41 (d, $^{1,4}J$ = 2.0, 1H; O*H*), 3.07 (t, ^{anti}J = 11.2, 1H; *H*C7), 2.95 (dd, ^{gem}J = 13.2, ^{gau}J = 2.2, 1H; ^{ax}*H*C2), 2.64 (m, ^{anti}J = 11.2, 10.4, plus unresolved couplings;1H; ^{ax}*H*C5), 2.51 (d, ^{syn}J = 10.4, 1H; ^{ax}*H*C6), 2.49–1.76 (m, 14H; mixed ring C*H* and C*H*), 1.69–1.52 (m, 3H; mixed CH_2), 1.35 (m, ^{gem}J = 13.2, plus unresolved couplings,1H; CH_2Ph), 1.23 (ddd, ^{anti}J = 10.4, ^{syn}J = 8.8, $^{1,4}J$ = 2.0, 1H; ^{ax}*H*C13), 1.18–1.04 (m, 2H; ring CH_2), 0.85–0.72 ppm (m, 1H; ring CH_2); ^{13}C NMR (100 MHz, $CDCl_3$): δ_C = 219.1, 213.4, 140.5, 129.1, 128.2, 125.9, 73.7, 55.9, 55.1, 45.0, 44.9, 43.1, 41.8, 41.4, 40.7, 35.6, 34.2, 31.5, 29.2, 28.2, 27.5, 20.7, 20.2 ppm; IR ($CHCl_3$): $\tilde{\nu}$ = 3605, 2934, 2864, 1703, 1600, 1454, 1391, 1004 cm^{-1}; HRMS (EI): calcd for $C_{25}H_{32}O_3Na^+$: 403.2249; found: 403.2244 $[M+Na]^+$.

X-ray crystal structure determination of 6b: Due to the very small size of the available crystals, it was necessary to collect diffraction data on Station 9.8 of the high-intensity Daresbury Synchrotron Radiation Source. Colourless needle, 0.08 × 0.01 × 0.01 mm^3, monoclinic, space group $P2_1/c$; *a* = 19.6178(13), *b* = 5.3724(4), *c* = 19.0540(12) Å; β = 97.207(2)°; *V* = 1992.3(2) Å^3; ρ_{calcd} = 1.269 g cm^{-3}; λ = 0.6727 Å; $2\theta_{max}$ = 60°; fine-slice ω scans; *T* = 120(2) K; 22629 reflections measured, 6374 unique (R_{int} = 0.041) used in refinement; corrections for Lorentz, polarisation and absorption (μ = 0.081 mm^{-1}, *T* range 0.993–0.999) effects were applied. The structure was solved by direct methods using SHELXS97[24] and refined

by full-matrix least squares using SHELXL97,[25] 254 parameters, H atoms placed geometrically and thereafter refined using a riding model, R_1 [4719 $F=4\sigma(F)$] = 0.0505, wR_2 [all 6375 F^2] = 0.144, refinement on F^2, $\Delta\rho_{max,\ min}$ = 0.37, −0.27 e Å^{-3}. CCDC-604125 contains the supplementary crystallographic data for this paper. These data can be obtained free of charge from The Cambridge Crystallographic Data Centre via www.ccdc.cam.ac.uk/data_request/cif.

Tetracycle 6f (R = $(CH_2)_3CO_2Et$): ^{1}H NMR (400 MHz, $CDCl_3$, 25 °C): δ_H = 4.38 (s, 1H; O*H*), 4.12 (qd, *J* = 7.2, 0.8, 2H), 2.98 (t, *J* = 11.2, 1H), 2.48–2.36 (m, 3H), 2.46 (d, *J* = 10.4, 1H), 2.33–2.21 (m, 4H), 2.18–2.02 (m, 2H), 2.05–1.38 (m, 14H), 1.26 (t, *J* = 7.2, 3H), 1.15–1.04 (m, 3H), 0.95–0.75 ppm (m, 2H); ^{13}C NMR (100 MHz, $CDCl_3$): δ_C = 219.1, 213.5, 173.6, 73.5, 60.3, 55.8, 55.0, 44.9, 44.7, 43.1, 41.8, 41.3, 34.6, 34.2, 33.8, 33.5, 31.6, 29.2, 28.2, 27.5, 21.9, 20.7, 20.3, 14.3 ppm; IR ($CHCl_3$): $\tilde{\nu}$ = 3505, 2936, 2864, 1709, 1602, 1455, 1372, 1045 cm^{-1}; HRMS (EI): calcd for $C_{24}H_{36}O_5^+$: 404.2563; found: 404.2568 $[M]^+$.

Preparation of $Zn(CH_2Ph)_2$: Literature preparations[18] of this compound were found to generate samples significantly contaminated with $PhCH_2ZnCl$, especially after exposure to 1,4-dioxane (as recommended[18]). The following procedure was found to be more reliable: A dried Schlenk tube under an argon atmosphere was charged with benzylmagnesium chloride (8.0 mL, 1.0 M Et_2O solution, 8.0 mmol), and $ZnCl_2$ (4.0 mL, 1.0 M Et_2O solution, 4.0 mmol) was added at RT over 10 min through a cannula to give a white suspension. The suspension was stirred for 24 h at RT and then filtered through Celite to give a 0.25 M colourless filtrate. ^{1}H NMR[18] (500 MHz, C_6D_6, 25 °C): δ_H = 7.32–7.28 (m, 2H), 7.25–7.21 (m, 2H), 7.02–6.98 (m, 1H), 2.05 ppm (s, 2H); ^{13}C NMR (125 MHz, C_6D_6): δ_C = 151.0, 127.9, 126.4, 119.7, 21.2 ppm.

Appendix

Derivation of Equation (5): Under the conditions of Equilibrium (2) the equilibrium constant is expected to be Equation (A1):

$$K = \frac{[ZnR_2][ZnX_2 \cdot MAO]}{[RZnX]^2[MAO]} \quad (A1)$$

As every turnover over of the equilibrium produces equimolar quantities of ZnR_2 and $[ZnBr_2{\cdot}MAO]$ then:

$$[ZnR_2] = [ZnX_2 \cdot MAO] \quad (A2)$$

The total amount of zinc in the system must be a constant, defining Equation (A3). By using the relationship given in Equation (A2) an expression for the concentration of RZnBr can be defined [Eq. (A4)]:

$$[Zn_{tot}] = [RZnX]+[ZnR_2]+[ZnX_2 \cdot MAO] \quad (A3)$$

$$[RZnX] = [Zn_{tot}]-2[ZnR_2] \quad (A4)$$

Similarly, the total amount of aluminium present in the system must be constant leading directly to Equations (A5) and (A6):

$$[Al_{tot}] = [MAO]+[ZnX_2 \cdot MAO] \quad (A5)$$

$$[Al_{tot}] = [MAO]+[ZnR_2] \quad (A6)$$

Substitution of Equations (A2), (A4) and (A6) into (A1) leads directly to Equation (5).

Derivation of Equation (4): Under the high temperature limit of Equation (A7) the observed chemical shift of the $ZnCH_2$ carbon must be the weighted average of the number of "R" groups in each environment allowing for the presence of two "R" groups in ZnR_2 leading to Equation (A8):

$$2\,RZnX+MAO \rightleftharpoons ZnR_2+ZnX_2 \cdot MAO \quad (A7)$$

$$\delta_{obs} = \frac{\delta_X[RZnX]+\delta_{R2}2[ZnR_2]}{[Zn_{tot}]} \quad (A8)$$

For which Equations (A3), (A4) and (A2) are all valid.

As:

$$[ZnR_2] = [ZnX_2 \cdot MAO] \quad (A2)$$

Therefore substituting Equation (A4) into (A8) leads directly to Equation (4).

Acknowledgements

This work was supported by the European Union Framework 6 Programme (Project: FP6-505267-1; LIGBANK, J.C.S.) and we thank the EPSRC-funded synchrotron crystallography service and its director Professor W. Clegg for collection of single-crystal diffraction data at Daresbury SRS Station 9.8. J.S. thanks the EPSRC for its contribution to a studentship. We acknowledge Dr. Chris Frost (University of Bath) for useful discussions.

[1] a) P. J. Goldsmith, S. Woodward, *Angew. Chem.* **2005**, *117*, 2275–2277; *Angew. Chem. Int. Ed.* **2005**, *44*, 2232–2234.
[2] Evans estimated $K < 0.002$ M based on the non-observation of $ZnEt_2$ in the ^{1}H NMR spectra of EtZnI; D. F. Evans, G. V. Fazakerley, *J. Chem. Soc. A* **1971**, 182–183.
[3] a) Boersma detected only EtZnCl in equimolar mixtures of $ZnEt_2$/$ZnCl_2$: J. Boersma, J. G. Noltes, *Tetrahedron Lett.* **1966**, *7*, 1521–1525; b) the species PhZnMe has been prepared in situ by admixture of $ZnPh_2$+$ZnMe_2$; P. I. Dosa, G. C. Fu, *J. Am. Chem. Soc.* **1998**, *120*, 445–446; c) P. I. Dosa, J. C. Ruble, G. C. Fu, *J. Org. Chem.* **1997**, *62*, 444–445.
[4] a) H. Yorimitsu, K. Oshima, *Angew. Chem.* **2005**, *117*, 4509–4513; *Angew. Chem. Int. Ed.* **2005**, *44*, 4435–4439.
[5] a) P. Knochel, J. J. A. Perea, P. Jones, *Tetrahedron* **1998**, *54*, 8275–8319; b) P. Knochel, P. Jones, *Organozinc Reagents: A Practical Approach*, Oxford Press, **1999**.
[6] a) R. I. Yousef, B. Walfort, T. Ruffer, C. Wagner, H. Schmidt, R. Herzog, D. Steinborn, *J. Organomet. Chem.* **2005**, *690*, 1178–1191; b) J. Tammiku-Taul, P. Burk, A. Tuulmets, *J. Phys. Chem. A* **2005**, *108*, 133–139; c) P. E. M. Allen, S. Hagiass, C. Mair, E. H. Williams, *Ber. Bunsen-Ges. Phys. Chem.* **1984**, *88*, 623–626.
[7] E. Zurek, T. Ziegler, *Prog. Polym. Sci.* **2004**, *29*, 107–148.
[8] a) For a review on inverse-crown chemistry see: R. E. Mulvey, *Organometallics* **2006**, *25*, 1060–1075; b) for information on anti-crown chemistry see: I. A. Tikhonova, K. I. Tugashov, F. M. Dolgushin, A. A. Yakovenko, B. N. Strunin, P. V. Petrovshii, G. G. Furin, V. B. Shur, *Inorg. Chim. Acta* **2006**, *359*, 2728–2735; c) V. B. Shur, I. A. Tikhonova, *Russ. Chem. Bull.* **2004**, *52*, 2539–2554.
[9] S. Woodward, *Tetrahedron* **2002**, *58*, 1017–1050.
[10] Y. Xiaoguang, Z. Zhiping, C. B. Knobler, M. F. Hawthorne, *J. Am. Chem. Soc.* **1993**, *115*, 193–195.
[11] a) A. R. Kennedy, R. E. Mulvey, R. B. Rowlings, *Angew. Chem.* **1998**, *110*, 3321- 3323; *Angew. Chem. Int. Ed.* **1998**, *37*, 3180–3183; b) A. R. Kennedy, R. E. Mulvey, B. A. Roberts, R. B. Rowlings, C. L. Raston, *Chem. Commun.* **1999**, 353–354.

[12] Attained by use of $K = 0.19$ in Equation (5), attaining [$ZnEt_2$] by use of the Excel "solver" function, see: J. E. Billio, *Excel for Chemists*, 2nd ed., Wiley, NY, **2001**.
[13] G. D. Allred, L. S. Liebeskind, *J. Am. Chem. Soc.* **1996**, *118*, 2748–2749.
[14] P. K. Fraser, S. Woodward, *Chem. Eur. J.* **2003**, *9*, 776–783.
[15] G. H. Posner, J. P. Mallomo, A. Y. Black, *Tetrahedron* **1981**, *37*, 3921–3926.
[16] R. L. Cargill, D. F. Bushey, J. J. Good, *J. Org. Chem.* **1979**, *44*, 300–301.
[17] L. I. Zakharkin, O. Y. Okhlobystin, *Izv. Akad. Nauk SSSR Ser. Khim.* **1963**, 193.
[18] V. Weissig, R. Beckhaus, U. Banasiak, T. H. Z Thiele, *Z. Anorg. Allg. Chem.* **1980**, *467*, 61.
[19] H. Nehl, W. R. Scheidt, *J. Organomet. Chem.* **1985**, *289*, 1–8.
[20] a) C. A. Ogle, J. B. Human, *Tetrahedron: Asymmetry* **2003**, *14*, 3281–3283; b) F. K. Zinn, E. C. Ramos, J. V. Comasseto, *Tetrahedron Lett.* **2001**, *42*, 2415–2417; c) P. Jones, C. K. Reddy, P. Knochel, *Tetrahedron* **1998**, *54*, 1471–1490; d) M. van Klaveren, E. S. M. Persson, D. M. Grove, J.-E. Bäckvall, G. van Koten, *Tetrahedron Lett.* **1994**, *35*, 5931–5934; e) B. H. Lipshutz, M. Koerner, D. A. Parker, *Tetrahedron Lett.* **1987**, *28*, 945–948; f) B. H. Lipshutz, J. A. Kozlowski, D. A. Parker, S. L. Nguyen, K. E. McCarthy, *J. Organomet. Chem.* **1985**, *285*, 437–447.
[21] M. P. Bertrand, L. Feray, R. Nouguier, P. Perfetti, *J. Org. Chem.* **1999**, *64*, 9189–9193.
[22] A. Yanagisawa, S. Habaue, K. Yasue, H. Yamamoto, *J. Am. Chem. Soc.* **1994**, *116*, 6130–6141.
[23] P. Knochel, P. Jones, C. K. Reddy, *Tetrahedron* **1998**, *54*, 1471–1490.
[24] G. M. Sheldrick, *Acta Crystallogr. Sect. A* **1990**, *46*, 467–473.
[25] SHELXL97, G. M. Sheldrick, University of Göttingen, Göttingen, Germany, **1998**.

Received: December 4, 2006
Published online: February 7, 2007

